Some analytical methods and appllications in electrical engineering

Serguei Maximov

Instituto Tecnológico de Morelia
Posgrado en Eléctrica

April 23, 2021

Introduction

Introduction

Maxwell's equations

Some analytical applications (linear case)

- Electromagnetic Field and Eddy Current Losses in Bushing Regions of Transformers
- Temperature distribution in the bushing region of tank wall

Introduction

Maxwell's equations

Some analytical applications (linear case)

- Electromagnetic Field and Eddy Current Losses in Bushing Regions of Transformers
- Temperature distribution in the bushing region of tank wall

Nonlinear problems

- Analytical model for nonlinear permeability. Effective nonlinear permeability
- Nonlinear permeability and nonlinear oscillations of the magnetic field.
- Electromagnetic Field and Eddy Current Losses in Bushing Regions of Transformers. Nonlinear problem.

Section

Electromagnetic devices

- Transformers

Electromagnetic devices

- Transformers

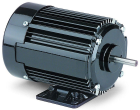

- Electric motors and generators

Electromagnetic devices

- Transformers

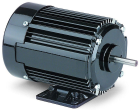

- Electric motors and generators

- Magnetic levitation systems

Electromagnetic devices

- Transformers

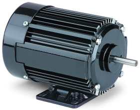

- Electric motors and generators

- Magnetic levitation systems

- Household appliances

Electromagnetic field distribution in transformers

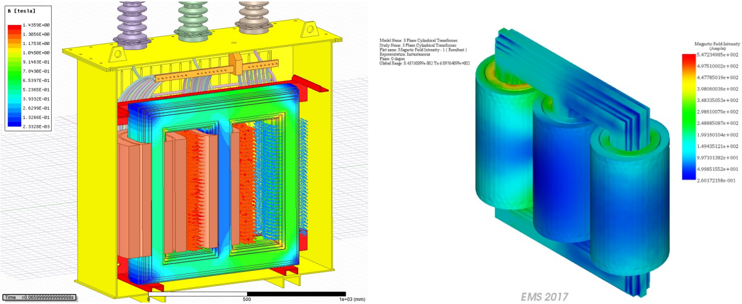

Figure 1: Magnetic field distribution in a transformer

Temperature distribution in transformers

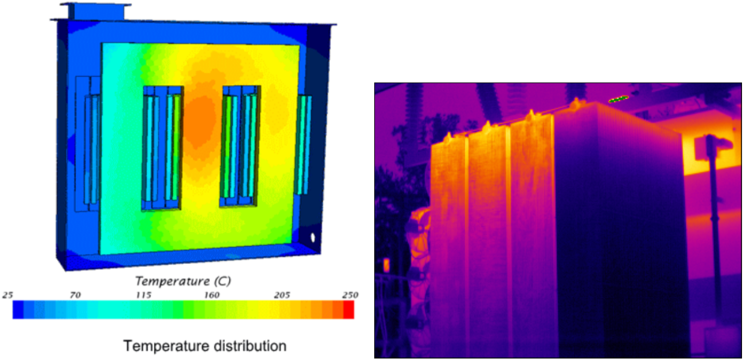

Figure 2: Calculated and measured temperature distribution in a transformer

Magnetic field distribution in electric motors

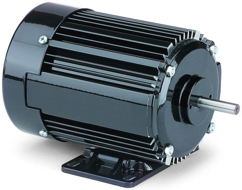

Figure 3: Electric motor

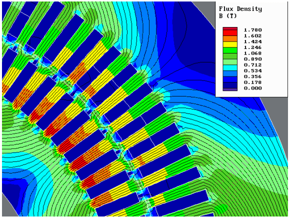

Figure 4: Magnetic field distribution in a motor core

Section

Maxwell's equations

James Clerk Maxwell

- "On Faraday's Lines of Force," *Transactions of the Cambridge Philosophical Society*, Vol. X, Part I., Dec. 10, 1855.

Maxwell's equations

James Clerk Maxwell

- "On Faraday's Lines of Force," *Transactions of the Cambridge Philosophical Society*, Vol. X, Part I., Dec. 10, 1855.

- "On Physical Lines of Force," *Philosophical Magazine*, Volume 21 & 23 Series 4, Part I & II; Part III & IV, 1861-1862.

Maxwell's equations

James Clerk Maxwell

- "On Faraday's Lines of Force," *Transactions of the Cambridge Philosophical Society*, Vol. X, Part I., Dec. 10, 1855.
- "On Physical Lines of Force," *Philosophical Magazine*, Volume 21 & 23 Series 4, Part I & II; Part III & IV, 1861-1862.

Modern form of Maxwell's equations (Heaviside, Hertz and Gibbs, 1884):

$$\nabla \cdot \mathbf{D} = \rho, \qquad \nabla \times \mathbf{E} = -\frac{\partial \mathbf{B}}{\partial t},$$
$$\nabla \cdot \mathbf{B} = 0, \quad \nabla \times \mathbf{H} = \mathbf{j} + \frac{\partial \mathbf{D}}{\partial t}.$$

Constitutive equations:

$$\mathbf{D} = \varepsilon_0 \varepsilon_{\mathrm{r}} \mathbf{E}, \qquad \mathbf{B} = \mu_0 \mu_{\mathrm{r}} \mathbf{H}.$$

Maxwell's equations. Low frequency approximation

Mainly, in the problems of electric engineering:

$$L \ll \lambda = \frac{c}{f}, \quad \Longrightarrow \quad f \ll \frac{c}{L}.$$

$\rho = 0$, $\mathbf{j} = \sigma \mathbf{E} + \mathbf{J}$.
In the low frequency limit:

$$\nabla \cdot \mathbf{D} = 0, \qquad \nabla \times \mathbf{E} = -\frac{\partial \mathbf{B}}{\partial t},$$

$$\nabla \cdot \mathbf{B} = 0, \quad \nabla \times \mathbf{H} = \sigma \mathbf{E} + \mathbf{J}.$$

Maxwell's equations. Low frequency approximation

Mainly, in the problems of electric engineering:

$$L \ll \lambda = \frac{c}{f}, \quad \Longrightarrow \quad f \ll \frac{c}{L}.$$

$\rho = 0$, $\mathbf{j} = \sigma \mathbf{E} + \mathbf{J}$.
In the low frequency limit:

$$\nabla \cdot \mathbf{D} = 0, \qquad \nabla \times \mathbf{E} = -\frac{\partial \mathbf{B}}{\partial t},$$

$$\nabla \cdot \mathbf{B} = 0, \quad \nabla \times \mathbf{H} = \sigma \mathbf{E} + \mathbf{J}.$$

Vector and scalar potentials:

$$\nabla \cdot \mathbf{B} = 0 \quad \Rightarrow \quad \mathbf{B} = \nabla \times \mathbf{A} \quad \Rightarrow \quad \nabla \times \left(\mathbf{E} + \frac{\partial \mathbf{A}}{\partial t} \right) = 0$$

Maxwell's equations. Low frequency approximation

Mainly, in the problems of electric engineering:

$$L \ll \lambda = \frac{c}{f}, \quad \Longrightarrow \quad f \ll \frac{c}{L}.$$

$\rho = 0$, $\mathbf{j} = \sigma \mathbf{E} + \mathbf{J}$.
In the low frequency limit:

$$\nabla \cdot \mathbf{D} = 0, \qquad \nabla \times \mathbf{E} = -\frac{\partial \mathbf{B}}{\partial t},$$
$$\nabla \cdot \mathbf{B} = 0, \quad \nabla \times \mathbf{H} = \sigma \mathbf{E} + \mathbf{J}.$$

Vector and scalar potentials:

$$\nabla \cdot \mathbf{B} = 0 \quad \Rightarrow \quad \mathbf{B} = \nabla \times \mathbf{A} \quad \Rightarrow \quad \nabla \times \left(\mathbf{E} + \frac{\partial \mathbf{A}}{\partial t} \right) = 0$$

$$\Rightarrow \quad \mathbf{E} + \frac{\partial \mathbf{A}}{\partial t} = -\nabla \varphi.$$

Thus,

$$\mathbf{E} = -\nabla \varphi - \frac{\partial \mathbf{A}}{\partial t}, \qquad \mathbf{B} = \nabla \times \mathbf{A}.$$

Maxwell's equations

In terms of magnetic field H:

$$\nabla \times \mathbf{H} = \sigma \mathbf{E} + \mathbf{J}$$

$$\nabla \times \nabla \times \mathbf{H} = \sigma \nabla \times \mathbf{E} + \nabla \times \mathbf{J}$$

Maxwell's equations

In terms of magnetic field H:

$$\nabla \times \mathbf{H} = \sigma \mathbf{E} + \mathbf{J}$$
$$\nabla \times \nabla \times \mathbf{H} = \sigma \nabla \times \mathbf{E} + \nabla \times \mathbf{J}$$

$$\left.\begin{aligned} \nabla \times \nabla \times \mathbf{H} &= \nabla \left(\nabla \cdot \mathbf{H} \right) - \nabla^2 \mathbf{H}, \\ \nabla \times \mathbf{E} &= -\frac{\partial \left(\mu_0 \mu_{\mathrm{r}} \mathbf{H} \right)}{\partial t}, \end{aligned}\right\} \Longrightarrow$$

Maxwell's equations

In terms of magnetic field H:

$$\nabla \times \mathbf{H} = \sigma \mathbf{E} + \mathbf{J}$$

$$\nabla \times \nabla \times \mathbf{H} = \sigma \nabla \times \mathbf{E} + \nabla \times \mathbf{J}$$

$$\left.\begin{aligned} &\nabla \times \nabla \times \mathbf{H} = \nabla\left(\nabla \cdot \mathbf{H}\right) - \nabla^2 \mathbf{H}, \\ &\nabla \times \mathbf{E} = -\frac{\partial\left(\mu_0 \mu_{\mathrm{r}} \mathbf{H}\right)}{\partial t}, \end{aligned}\right\} \Longrightarrow$$

$$\nabla\left(\nabla \cdot \mathbf{H}\right) - \nabla^2 \mathbf{H} = -\frac{\partial\left(\mu_0 \mu_{\mathrm{r}} \mathbf{H}\right)}{\partial t} + \nabla \times \mathbf{J}.$$

Section

Introduction

Maxwell's equations

Some analytical applications (linear case)

- Electromagnetic Field and Eddy Current Losses in Bushing Regions of Transformers
- Temperature distribution in the bushing region of tank wall

Nonlinear problems

- Analytical model for nonlinear permeability. Effective nonlinear permeability
- Nonlinear permeability and nonlinear oscillations of the magnetic field.
- Electromagnetic Field and Eddy Current Losses in Bushing Regions of Transformers. Nonlinear problem.

Bushing region of transformer

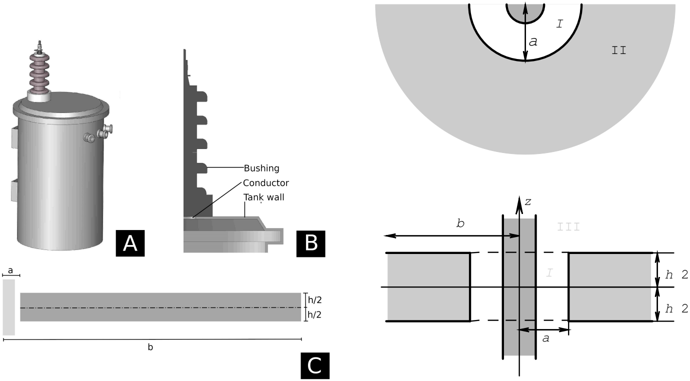

Figure 5: Bushing region of a transformer

Bushing region of transformer

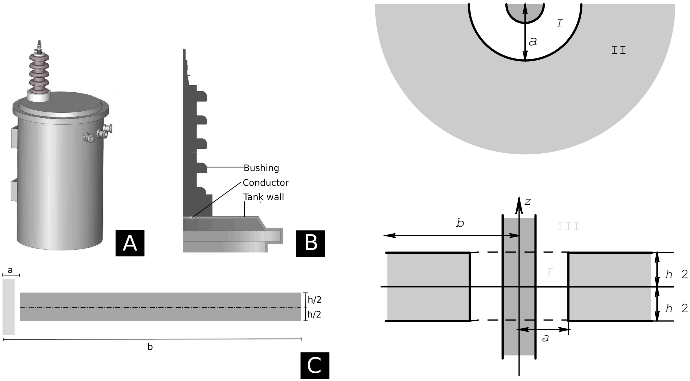

Figure 5: Bushing region of a transformer

AC in the conductor: $I(t) = \mathrm{Re}\{Ie^{j\omega t}\}$,

Bushing region of transformer

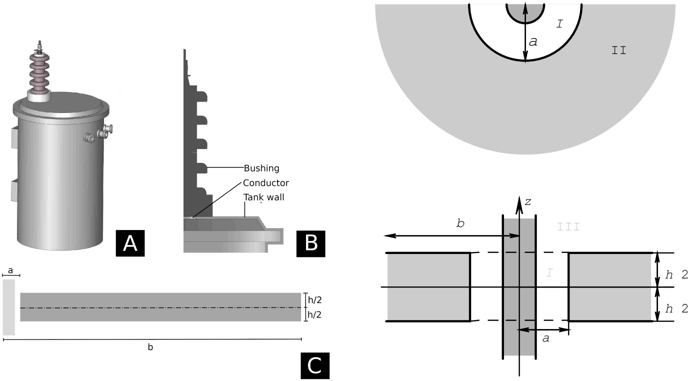

Figure 5: Bushing region of a transformer

AC in the conductor: $I(t) = \mathrm{Re}\{Ie^{j\omega t}\}$,
where I is the amplitude.

Magnetic field inside the tank wall

Axial symmetry $\Longrightarrow$ Cylindrical coordinates

Magnetic field inside the tank wall

Axial symmetry $\Longrightarrow$ Cylindrical coordinates

In the frequency domain:

$$\begin{cases} \frac{1}{r}\frac{\partial}{\partial r}\left(r\frac{\partial H}{\partial r}\right) + \frac{\partial^2 H}{\partial z^2} - \frac{H}{r^2} - \beta^2 H = 0, \\ H(r, \pm h/2) = \frac{I}{2\pi r}, \\ H(a, z) = \frac{I}{2\pi a}, \end{cases}$$

where $\beta^2 = j\omega\mu\sigma$.

Magnetic field inside the tank wall

Axial symmetry $\Longrightarrow$ Cylindrical coordinates

In the frequency domain:

$$\begin{cases} \dfrac{1}{r}\dfrac{\partial}{\partial r}\left(r\dfrac{\partial H}{\partial r}\right)+\dfrac{\partial^2 H}{\partial z^2}-\dfrac{H}{r^2}-\beta^2 H=0, \\ H(r,\pm h/2)=\dfrac{I}{2\pi r}, \\ H(a,z)=\dfrac{I}{2\pi a}, \end{cases}$$

where $\beta^2 = j\omega\mu\sigma$.

Analytical solution:

$$H(r,z)=\frac{I}{2\pi a}\left\{\frac{a}{r}\frac{\cosh(\beta z)}{\cosh(\beta h/2)} + \frac{4\beta^2}{\pi}\sum_{n=0}^{\infty}\frac{(-1)^n}{\lambda_n^2(2n+1)}\frac{K_1(\lambda_n r)}{K_1(\lambda_n a)}\cos\left(\frac{\pi(2n+1)}{h}z\right)\right\},$$

Magnetic field inside the tank wall

Axial symmetry $\Longrightarrow$ Cylindrical coordinates

In the frequency domain:

$$\begin{cases} \dfrac{1}{r}\dfrac{\partial}{\partial r}\left(r\dfrac{\partial H}{\partial r}\right) + \dfrac{\partial^2 H}{\partial z^2} - \dfrac{H}{r^2} - \beta^2 H = 0, \\ H(r, \pm h/2) = \dfrac{I}{2\pi r}, \\ H(a, z) = \dfrac{I}{2\pi a}, \end{cases}$$

where $\beta^2 = j\omega\mu\sigma$.

Analytical solution:

$$H(r,z) = \frac{I}{2\pi a}\left\{ \frac{a}{r}\frac{\cosh(\beta z)}{\cosh(\beta h/2)} + \frac{4\beta^2}{\pi}\sum_{n=0}^{\infty}\frac{(-1)^n}{\lambda_n^2(2n+1)}\frac{K_1(\lambda_n r)}{K_1(\lambda_n a)}\cos\left(\frac{\pi(2n+1)}{h}z\right)\right\},$$

where $\lambda^2 = \beta^2 + \left(\dfrac{\pi(2n+1)}{h}z\right)^2$, $n = 0, 1, 2, \ldots$.

Electric field inside the tank wall

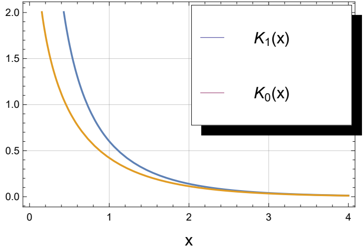

Figure 6: Modified Bessel functions $K_1(x)$ and $K_0(x)$.

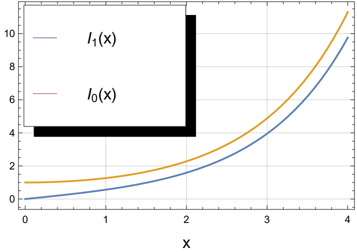

Figure 7: Modified Bessel functions $I_1(x)$ and $I_0(x)$.

Electric field inside the tank wall

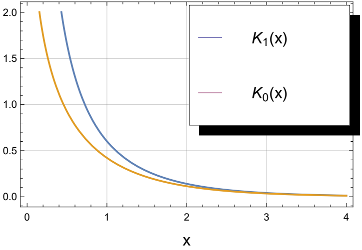

Figure 6: Modified Bessel functions $K_1(x)$ and $K_0(x)$.

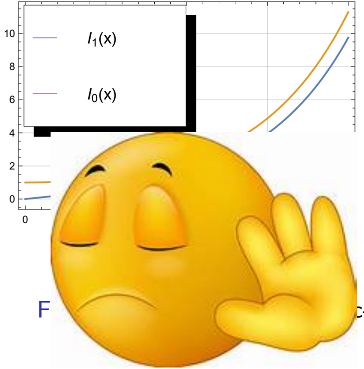

F

c-

Electric field inside the tank wall

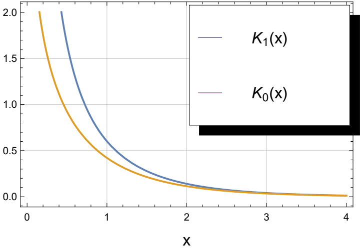

Figure 6: Modified Bessel functions $K_1(x)$ and $K_0(x)$.

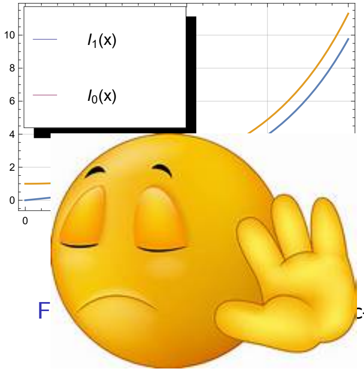

F [illegible] c-

$$E_r(r,z) = -\frac{\beta}{\sigma}\frac{I}{2\pi a}\left\{\frac{a}{r}\frac{\sinh(\beta z)}{\cosh(\beta h/2)} - \frac{4\beta}{h}\sum_{n=0}^{\infty}\frac{(-1)^n}{\lambda_n^2}\frac{K_1(\lambda_n r)}{K_1(\lambda_n a)}\sin\left(\frac{\pi(2n+1)}{h}z\right)\right\}.$$

Electric field inside the tank wall

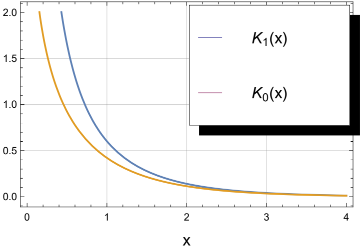

Figure 6: Modified Bessel functions $K_1(x)$ and $K_0(x)$.

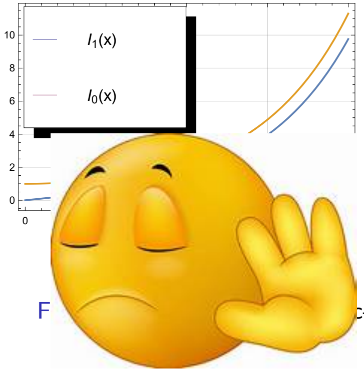

$$E_r(r,z) = -\frac{\beta}{\sigma}\frac{I}{2\pi a}\left\{\frac{a}{r}\frac{\sinh(\beta z)}{\cosh(\beta h/2)} - \frac{4\beta}{h}\sum_{n=0}^{\infty}\frac{(-1)^n}{\lambda_n^2}\frac{K_1(\lambda_n r)}{K_1(\lambda_n a)}\sin\left(\frac{\pi(2n+1)}{h}z\right)\right\}.$$

$$E_z(r,z) = -\frac{4\beta^2}{\pi\sigma}\frac{I}{2\pi a}\sum_{n=0}^{\infty}\frac{(-1)^n}{\lambda_n(2n+1)}\frac{K_0(\lambda_n r)}{K_1(\lambda_n a)}\cos\left(\frac{\pi(2n+1)}{h}z\right)$$

Magnetic field penetration into the tank wall

Figure 8: Magnetic field penetration in the tank wall for $\mu_r = 200$. Case 1. $\sigma = 4 \times 10^6\,(\Omega m)^{-1}$. Case 2. $\sigma = 1.33 \times 10^6\,(\Omega m)^{-1}$.

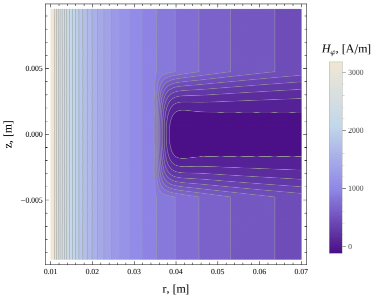

a)

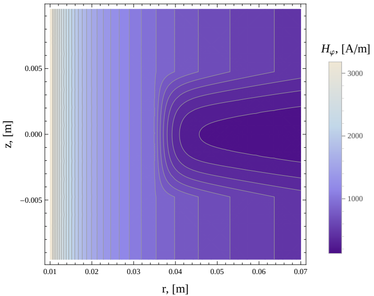

a)

Electric field distribution in the tank wall

Figure 9: Electric field distribution in the tank wall for $\mu_{\mathrm{r}} = 200$. Case 1. $\sigma = 4 \times 10^6\,(\Omega m)^{-1}$. Case 2. $\sigma = 1.33 \times 10^6\,(\Omega m)^{-1}$.

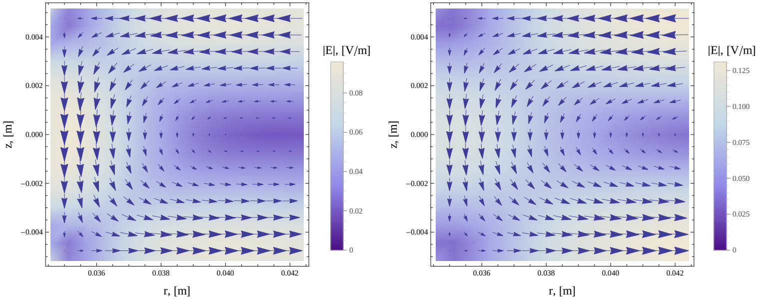

a)　　**a**)

Power losses density in the tank wall

Eddy current losses in the tank wall (average per period of oscillations T):

$$W(r,z) = \frac{1}{T}\int_0^T \sigma \mathbf{E}^2(r,z,t)dt = \frac{1}{2}\sigma\left(|E_r(r,z)|^2 + |E_z(r,z)|^2\right).$$

Figure 10: Power losses distribution in the tank wall for $\mu_{\mathrm{r}} = 200$. Case 1. $\sigma = 4\times 10^6\,(\Omega m)^{-1}$. Case 2. $\sigma = 1.33\times 10^6\,(\Omega m)^{-1}$.

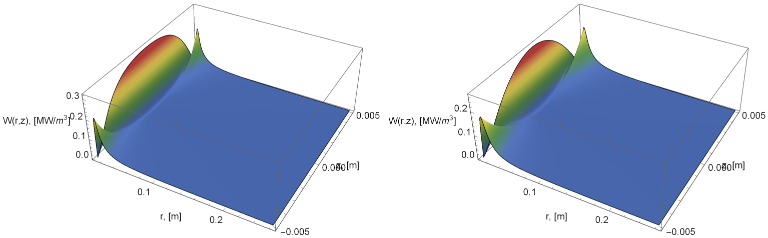

Power losses density in the center of the tank wall

Figure 11: Power losses density in the center of the tank wall for $\mu_r = 200$. Case 1. $\sigma = 4 \times 10^6\, (\Omega m)^{-1}$. Case 2. $\sigma = 1.33 \times 10^6\, (\Omega m)^{-1}$.

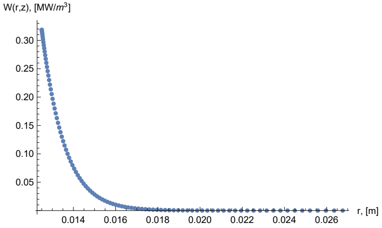

Temperature distribution in the tank wall

Heat equation: $\frac{1}{r}\frac{\partial}{\partial r}\left(r\frac{\partial T}{\partial r}\right)+\frac{\partial^2 T}{\partial z^2}=-\frac{1}{k_t}W(r,z).$

Boundary conditions:

$$\left.\left(k_t\frac{\partial T}{\partial r}-h_{c1}\left(T-T_{a1}\right)\right)\right|_{r=a}=0,\qquad \left.\left(k_t\frac{\partial T}{\partial r}+h_{c2}\left(T-T_{a2}\right)\right)\right|_{r=b}=0,$$

$$\left.\left(k_t\frac{\partial T}{\partial z}+h_{c3}\left(T-T_{a3}\right)\right)\right|_{z=\frac{h}{2}}=0,\qquad \left.\left(k_t\frac{\partial T}{\partial z}-h_{c4}\left(T-T_{a4}\right)\right)\right|_{z=-\frac{h}{2}}=0.$$

Temperature distribution in the tank wall

Heat equation: $\frac{1}{r}\frac{\partial}{\partial r}\left(r\frac{\partial T}{\partial r}\right)+\frac{\partial^2 T}{\partial z^2}=-\frac{1}{k_t}W(r,z).$

Boundary conditions:

$$\left(k_t\frac{\partial T}{\partial r}-h_{c1}\left(T-T_{a1}\right)\right)\bigg|_{r=a}=0,\quad \left(k_t\frac{\partial T}{\partial r}+h_{c2}\left(T-T_{a2}\right)\right)\bigg|_{r=b}=0,$$
$$\left(k_t\frac{\partial T}{\partial z}+h_{c3}\left(T-T_{a3}\right)\right)\bigg|_{z=\frac{h}{2}}=0,\quad \left(k_t\frac{\partial T}{\partial z}-h_{c4}\left(T-T_{a4}\right)\right)\bigg|_{z=-\frac{h}{2}}=0.$$

Parameters	Values	Parameters	Values
μ_{r}	500	h_{c4}	$35\,\mathrm{W/m^2K}$
k_t	$16\,\mathrm{W/mK}$	T_{a1}	$80\,^\circ\mathrm{C}$
f	$50\,\mathrm{s}^{-1}$	T_{a2}	$18\,^\circ\mathrm{C}$
h_{c1}	$25\,\mathrm{W/m^2K}$	T_{a3}	$18\,^\circ\mathrm{C}$
h_{c2}	$10\,\mathrm{W/m^2K}$	T_{a4}	$80\,^\circ\mathrm{C}$
h_{c3}	$10\,\mathrm{W/m^2K}$		

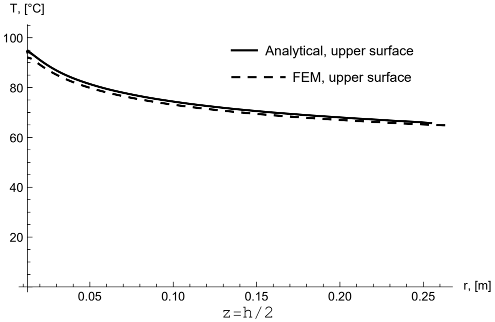

Figure 12: Temperature profiles on the upper surface.

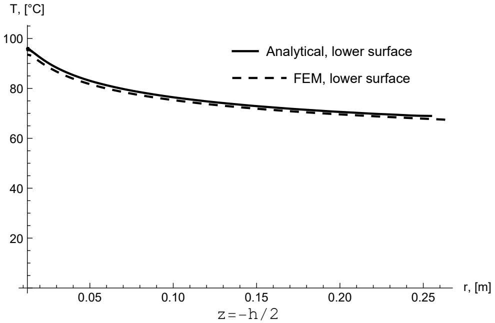

Figure 13: Temperature profiles on the lower surface.

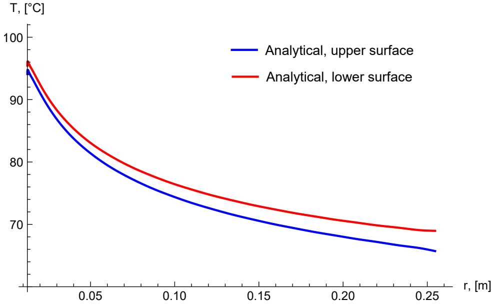

Figure 14: Temperature profiles on the upper and lower surfaces. Vertical temperature gradient.

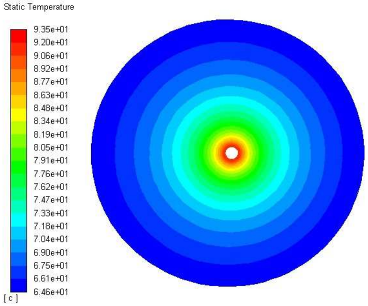

Figure 15: 2D temperature distribution. FEM-simulations.

- FEM requires considerable time-consuming computational resources, especially when dealing with 3D geometries and very pronounced skin-effects, where a high density meshing is normally required.

- FEM requires considerable time-consuming computational resources, especially when dealing with 3D geometries and very pronounced skin-effects, where a high density meshing is normally required.
- Analytical formulae provide high precision results such as:

- FEM requires considerable time-consuming computational resources, especially when dealing with 3D geometries and very pronounced skin-effects, where a high density meshing is normally required.
- Analytical formulae provide high precision results such as:
  - distribution of eddy current losses in transformer tanks and cores

- FEM requires considerable time-consuming computational resources, especially when dealing with 3D geometries and very pronounced skin-effects, where a high density meshing is normally required.
- Analytical formulae provide high precision results such as:
  - distribution of eddy current losses in transformer tanks and cores
  - estimation of temperature distributions in the vital parts of transformers

- FEM requires considerable time-consuming computational resources, especially when dealing with 3D geometries and very pronounced skin-effects, where a high density meshing is normally required.
- Analytical formulae provide high precision results such as:
  - distribution of eddy current losses in transformer tanks and cores
  - estimation of temperature distributions in the vital parts of transformers
  - prediction and estimation of hot spots and other hazards

- FEM requires considerable time-consuming computational resources, especially when dealing with 3D geometries and very pronounced skin-effects, where a high density meshing is normally required.
- Analytical formulae provide high precision results such as:
  - distribution of eddy current losses in transformer tanks and cores
  - estimation of temperature distributions in the vital parts of transformers
  - prediction and estimation of hot spots and other hazards
- Analytical method do not need of expensive computational resources.

Section

Introduction

Maxwell's equations

Some analytical applications (linear case)

- Electromagnetic Field and Eddy Current Losses in Bushing Regions of Transformers
- Temperature distribution in the bushing region of tank wall

Nonlinear problems

- Analytical model for nonlinear permeability. Effective nonlinear permeability
- Nonlinear permeability and nonlinear oscillations of the magnetic field.
- Electromagnetic Field and Eddy Current Losses in Bushing Regions of Transformers. Nonlinear problem.

Maxwell's equations in media with nonlinear permeability

$$\begin{cases} \dfrac{1}{r}\dfrac{\partial}{\partial r}\left(r\dfrac{\partial H}{\partial r}\right) + \dfrac{\partial^2 H}{\partial z^2} - \dfrac{H}{r^2} - \sigma\dfrac{\partial(\mu H)}{\partial t} = 0, \\ H(r, \pm h/2) = \dfrac{I}{2\pi r}, \\ H(a, z) = \dfrac{I}{2\pi a}, \end{cases}$$

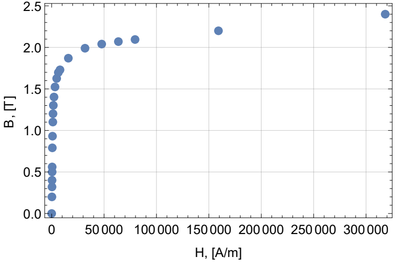

Figure 16: Magnetization points for 1010 low carbon steel.

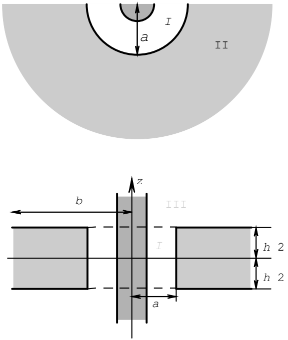

Figure 17: Bushing region of a transformer

Analytical approximation for nonlinear permeability.

Analytical approximation for nonlinear permeability.

Analytical calculations need of an analytical form of the magnetization curve.

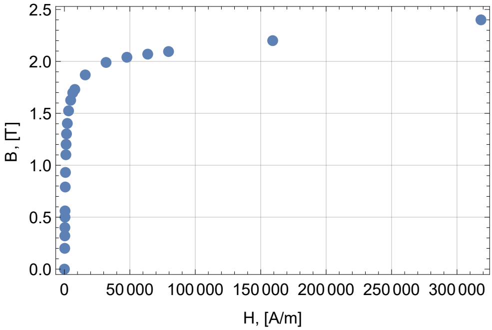

Figure 18: Magnetization points for 1010 low carbon steel.

Analytical approximation for nonlinear permeability.

Analytical calculations need of an analytical form of the magnetization curve.

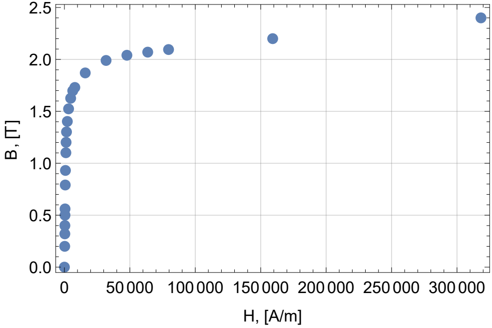

Figure 18: Magnetization points for 1010 low carbon steel.

$$B = \mu_0 \left(\gamma_1 \arctan(\gamma_2 H) + \gamma_3 H \right),$$

where γ_1, γ_2 and γ_3 are constants to be obtained from experimental points.

Analytical approximation for nonlinear permeability.

Least squares method minimizes the sum of the squared errors:

Analytical approximation for nonlinear permeability.

Least squares method minimizes the sum of the squared errors:

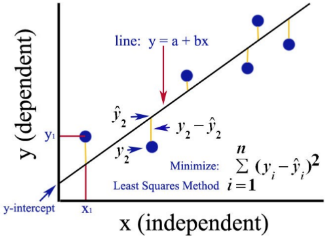

Figure 19: Least squares method minimizes the sum of the squared errors.

Analytical approximation for nonlinear permeability.

Least squares method minimizes the sum of the squared errors:

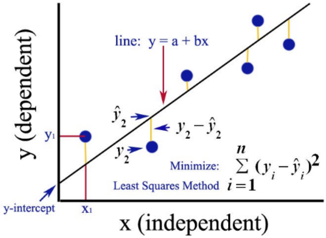

Figure 19: Least squares method minimizes the sum of the squared errors.

To be minimized:

$$L[\gamma_1, \gamma_2, \gamma_3] = \sum_{k=1}^{N} \left\{ B_k - \mu_0 \left(\gamma_1 \arctan(\gamma_2 H_k) + \gamma_3 H_k \right) \right\}^2.$$

Analytical approximation for nonlinear permeability.

Least squares method minimizes the sum of the squared errors:

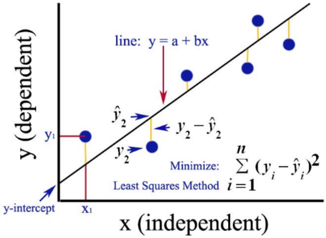

Figure 19: Least squares method minimizes the sum of the squared errors.

To be minimized:

$$L[\gamma_1, \gamma_2, \gamma_3] = \sum_{k=1}^{N} \left\{ B_k - \mu_0 \left(\gamma_1 \arctan(\gamma_2 H_k) + \gamma_3 H_k \right) \right\}^2.$$

The result of minimization:

$$\gamma_1 = 999637.86 \, \mathrm{A/m}$$
$$\gamma_2 = 0.001002 \, (\mathrm{A/m})^{-1}$$
$$\gamma_3 = 1.0861$$

Analytical approximation for nonlinear permeability.

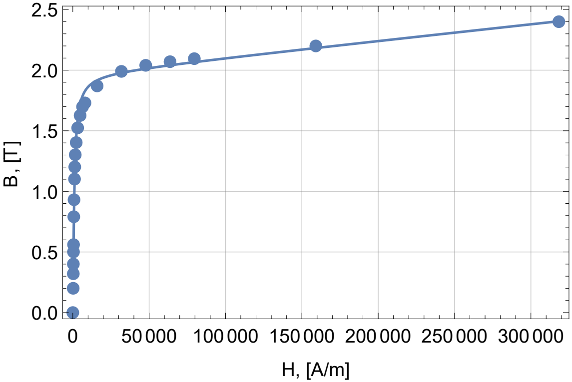

Figure 20: Magnetization curve: analytical result vs. experimental points.

Relative error $< 1\%$.

Nonlinear oscillations.

Consider the magnetic field of harmonic form:
$H = H_1 e^{j\omega t} + H_{-1} e^{-j\omega t}, \qquad \text{where } H_1 \in \mathbb{C}.$

Nonlinear oscillations.

Consider the magnetic field of harmonic form:
$H = H_1 e^{j\omega t} + H_{-1} e^{-j\omega t}$, where $H_1 \in \mathbb{C}$.

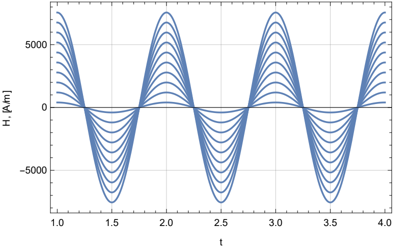

Figure 21: Harmonic oscillations of H

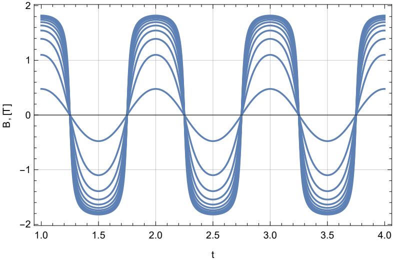

Figure 22: Nonlinear oscillations of B

Nonlinear oscillations.

Consider the magnetic field of harmonic form:
$H = H_1 e^{j\omega t} + H_{-1} e^{-j\omega t}$, where $H_1 \in \mathbb{C}$.

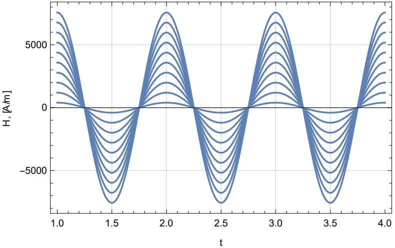

Figure 21: Harmonic oscillations of H

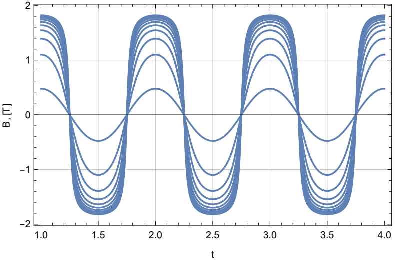

Figure 22: Nonlinear oscillations of B

Oscillations in a nonlinear system lead to appearance of higher harmonics

Nonlinear permeability: Fourier expansion

$$H(t) = H_1 e^{j\omega t} + H_{-1} e^{-j\omega t}$$

$\longrightarrow$

$$B(t) = \mu_0 \left(\gamma_1 \arctan(\gamma_2 H(t)) + \gamma_3 H(t)\right)$$

$\downarrow$

Expansion in a Fourier series

Nonlinear permeability: Fourier expansion

$$H(t) = H_1 e^{j\omega t} + H_{-1} e^{-j\omega t}$$

$\longrightarrow$

$$B(t) = \mu_0 \left(\gamma_1 \arctan(\gamma_2 H(t)) + \gamma_3 H(t)\right)$$

$\downarrow$

Expansion in a Fourier series

Complex Fourier series:

$$B(t) = \sum_{n=-\infty}^{+\infty} B_n e^{jn\omega t},$$

Nonlinear permeability: Fourier expansion

$$H(t) = H_1 e^{j\omega t} + H_{-1} e^{-j\omega t}$$

$\longrightarrow$ $B(t) = \mu_0 \left(\gamma_1 \arctan(\gamma_2 H(t)) + \gamma_3 H(t)\right)$

$\downarrow$

Expansion in a Fourier series

Complex Fourier series:

$$B(t) = \sum_{n=-\infty}^{+\infty} B_n e^{jn\omega t},$$

where

$$B_n = \frac{\omega}{2\pi} \int_0^{2\pi/\omega} \mu_0 \left(\gamma_1 \arctan(\gamma_2 H(t)) + \gamma_3 H(t)\right) dt.$$

Nonlinear permeability: Fourier expansion

$$H(t) = H_1 e^{j\omega t} + H_{-1} e^{-j\omega t}$$

$\longrightarrow$ $B(t) = \mu_0 \left(\gamma_1 \arctan(\gamma_2 H(t)) + \gamma_3 H(t)\right)$

$\downarrow$

Expansion in a Fourier series

Complex Fourier series:

$$+\infty$$

where

$$B_n = \frac{\omega}{2\pi} \int \; \ldots \; t))\, dt.$$

Nonlinear permeability: Fourier expansion

Nonlinear permeability: Fourier expansion

$$H = H_1 e^{j\omega t} + H_{-1} e^{-j\omega t}$$

$\longrightarrow$

$$\frac{\partial B}{\partial t} = \mu_0 \left(\frac{\gamma_1 \gamma_2}{1 + (\gamma_2 H)^2} + \gamma_3 \right) \frac{\partial H}{\partial t}$$

$\downarrow$

Expansion in a power series with respect to $e^{j\omega t}$

$\downarrow$

Reconstruction of $B(t)$:

$$B(t) = \int \frac{\partial B}{\partial t} dt + C$$

Nonlinear permeability: Fourier expansion

$$H = H_1 e^{j\omega t} + H_{-1} e^{-j\omega t}$$

$\longrightarrow$

$$\frac{\partial B}{\partial t} = \mu_0 \left(\frac{\gamma_1 \gamma_2}{1 + (\gamma_2 H)^2} + \gamma_3 \right) \frac{\partial H}{\partial t}$$

$\downarrow$

Expansion in a power series with respect to $e^{j\omega t}$

$\downarrow$

Reconstruction of $B(t)$:

$$B(t) = \int \frac{\partial B}{\partial t} dt + C$$

$$\frac{1}{1+(\gamma_2 H)^2} = \frac{1}{1+(\gamma_2 H_1 e^{j\omega t} + \gamma_2 H_{-1} e^{-j\omega t})^2}$$

$$= \frac{1}{1+2|\gamma_2 H_1|^2 + (\gamma_2 H_1)^2 e^{2j\omega t} + (\gamma_2 H_{-1})^2 e^{-2j\omega t}},$$

$$\frac{1}{1+(\gamma_2 H)^2} = \frac{1}{1+(\gamma_2 H_1 e^{j\omega t} + \gamma_2 H_{-1} e^{-j\omega t})^2}$$

$$= \frac{1}{1+2|\gamma_2 H_1|^2 + (\gamma_2 H_1)^2 e^{2j\omega t} + (\gamma_2 H_{-1})^2 e^{-2j\omega t}},$$

where

$$1+2|\gamma_2 H_1|^2 > \left|(\gamma_2 H_1)^2 e^{2j\omega t} + (\gamma_2 H_{-1})^2 e^{-2j\omega t}\right|$$

$$\frac{1}{1+(\gamma_2 H)^2} = \frac{1}{1+\left(\gamma_2 H_1 e^{j\omega t} + \gamma_2 H_{-1} e^{-j\omega t}\right)^2}$$

$$= \frac{1}{1+2|\gamma_2 H_1|^2 + (\gamma_2 H_1)^2 e^{2j\omega t} + (\gamma_2 H_{-1})^2 e^{-2j\omega t}},$$

where

$$1+2|\gamma_2 H_1|^2 > \left|(\gamma_2 H_1)^2 e^{2j\omega t} + (\gamma_2 H_{-1})^2 e^{-2j\omega t}\right|$$

This allows expansion in a geometric progression:

$$\frac{1}{a+z} = \sum_{n=0}^{\infty} \frac{(-1)^n}{a^{n+1}} z^n \quad \text{if} \quad |a| > |z|.$$

$$\frac{1}{1+(\gamma_2 H)^2} = \frac{1}{1+\left(\gamma_2 H_1 e^{j\omega t} + \gamma_2 H_{-1} e^{-j\omega t}\right)^2}$$
$$= \frac{1}{1+2|\gamma_2 H_1|^2 + (\gamma_2 H_1)^2 e^{2j\omega t} + (\gamma_2 H_{-1})^2 e^{-2j\omega t}},$$

where

$$1+2|\gamma_2 H_1|^2 > \left|(\gamma_2 H_1)^2 e^{2j\omega t} + (\gamma_2 H_{-1})^2 e^{-2j\omega t}\right|$$

This allows expansion in a geometric progression:

$$\frac{1}{a+z} = \sum_{n=0}^{\infty} \frac{(-1)^n}{a^{n+1}} z^n \quad \text{if} \quad |a| > |z|.$$

$$\frac{1}{1+(\gamma_2 H)^2} \frac{\partial H}{\partial t} = j\omega \left(H_1 e^{j\omega t} - H_{-1} e^{-j\omega t}\right)$$
$$\times \sum_{n=0}^{\infty} \frac{(-1)^n \left[(\gamma_2 H_1)^2 e^{2j\omega t} + (\gamma_2 H_{-1})^2 e^{-2j\omega t}\right]^n}{\left(1+2|\gamma_2 H_1|^2\right)^{n+1}}$$

$$\frac{1}{1+(\gamma_2 H)^2} = \frac{1}{1+\left(\gamma_2 H_1 e^{j\omega t} + \gamma_2 H_{-1} e^{-j\omega t}\right)^2}$$

$$= \frac{1}{1+2|\gamma_2 H_1|^2 + (\gamma_2 H_1)^2 e^{2j\omega t} + (\gamma_2 H_{-1})^2 e^{-2j\omega t}},$$

where

$$1+2|\gamma_2 H_1|^2 > \left|(\gamma_2 H_1)^2 e^{2j\omega t} + (\gamma_2 H_{-1})^2 e^{-2j\omega t}\right|$$

This allows expansion in a geometric progression:

$$\frac{1}{a+z} = \sum_{n=0}^{\infty} \frac{(-1)^n}{a^{n+1}} z^n \quad \text{if} \quad |a| > |z|.$$

$$\frac{1}{1+(\gamma_2 H)^2}\frac{\partial H}{\partial t} = j\omega\left(H_1 e^{j\omega t} - H_{-1} e^{-j\omega t}\right)$$

$$\times \sum_{n=0}^{\infty} \frac{(-1)^n \left[(\gamma_2 H_1)^2 e^{2j\omega t} + (\gamma_2 H_{-1})^2 e^{-2j\omega t}\right]^n}{\left(1+2|\gamma_2 H_1|^2\right)^{n+1}}$$

$$(x+y)^n = \sum_{m=0}^{n} C_n^m x^m y^{n-m}, \quad \text{where} \quad C_n^m = \frac{n!}{m!(n-m)!}.$$

$$
\begin{aligned}
&\frac{1}{1+(\gamma_2 H)^2}\frac{\partial H}{\partial t} \\
&= \sum_{k=0}^{\infty}(-1)^k j\omega\left[H_1(\gamma_2 H_1)^{2k}e^{(2k+1)j\omega t} - H_{-1}(\gamma_2 H_{-1})^{2k}e^{-(2k+1)j\omega t}\right] \\
&\times \sum_{m=0}^{\infty}\left[\frac{C_{2m+k}^{m}|\gamma_2 H_1|^{4m}}{(1+2|\gamma_2 H_1|^2)^{2m+k+1}} + \frac{C_{2m+k+1}^{m}|\gamma_2 H_1|^{2(2m+1)}}{(1+2|\gamma_2 H_1|^2)^{2m+k+2}}\right],
\end{aligned}
$$

$$
\begin{aligned}
&\frac{1}{1+(\gamma_2 H)^2}\frac{\partial H}{\partial t} \\
&= \sum_{k=0}^{\infty}(-1)^k j\omega\left[H_1(\gamma_2 H_1)^{2k}e^{(2k+1)j\omega t} - H_{-1}(\gamma_2 H_{-1})^{2k}e^{-(2k+1)j\omega t}\right] \\
&\times \sum_{m=0}^{\infty}\left[\frac{C_{2m+k}^{m}|\gamma_2 H_1|^{4m}}{(1+2|\gamma_2 H_1|^2)^{2m+k+1}} + \frac{C_{2m+k+1}^{m}|\gamma_2 H_1|^{2(2m+1)}}{(1+2|\gamma_2 H_1|^2)^{2m+k+2}}\right],
\end{aligned}
$$

where

$$
\begin{aligned}
&\frac{1}{1+(\gamma_2 H)^2}\frac{\partial H}{\partial t} \\
&= \sum_{k=0}^{\infty}(-1)^k j\omega\left[H_1(\gamma_2 H_1)^{2k}e^{(2k+1)j\omega t} - H_{-1}(\gamma_2 H_{-1})^{2k}e^{-(2k+1)j\omega t}\right] \\
&\times \sum_{m=0}^{\infty}\left[\frac{C_{2m+k}^{m}|\gamma_2 H_1|^{4m}}{(1+2|\gamma_2 H_1|^2)^{2m+k+1}} + \frac{C_{2m+k+1}^{m}|\gamma_2 H_1|^{2(2m+1)}}{(1+2|\gamma_2 H_1|^2)^{2m+k+2}}\right],
\end{aligned}
$$

where

$$
\begin{aligned}
&\sum_{m=0}^{\infty}\left[\frac{C_{2m+k}^{m}z^{4m}}{(1+2z^2)^{2m+k+1}} + \frac{C_{2m+k+1}^{m}z^{2(2m+1)}}{(1+2z^2)^{2m+k+2}}\right] \\
&= \frac{\sqrt{1+4z^2}-1}{2z^2}\frac{2^k}{\left[1+2z^2+\sqrt{1+4z^2}\right]^k}.
\end{aligned}
$$

Finally,

$$
\begin{aligned}
\frac{\partial B}{\partial t} &= \mu_0 \left(\frac{\gamma_1 \gamma_2}{1+(\gamma_2 H)^2} + \gamma_3 \right) \frac{\partial H}{\partial t} \\
&= \mu_0 \gamma_1 \gamma_2 \frac{\sqrt{1+4|\gamma_2 H_1|^2}-1}{2|\gamma_2 H_1|^2} \\
&\times \sum_{k=0}^{\infty} j\omega \left[H_1 (\gamma_2 H_1)^{2k} e^{(2k+1)j\omega t} - H_{-1} (\gamma_2 H_{-1})^{2k} e^{-(2k+1)j\omega t} \right] \\
&\times (-2)^k \left[1 + 2|\gamma_2 H_1|^2 + \sqrt{1+4|\gamma_2 H_1|^2} \right]^{-k}, \\
&+ \mu_0 \gamma_3 j\omega \left(H_1 e^{j\omega t} - H_{-1} e^{-j\omega t} \right)
\end{aligned}
$$

Finally,

$$\frac{\partial B}{\partial t} = \mu_0 \left(\frac{\gamma_1 \gamma_2}{1 + (\gamma_2 H)^2} + \gamma_3 \right) \frac{\partial H}{\partial t}$$

$$= \mu_0 \gamma_1 \gamma_2 \frac{\sqrt{1 + 4|\gamma_2 H_1|^2} - 1}{2|\gamma_2 H_1|^2}$$

$$\times \sum_{k=0}^{\infty} j\omega \left[H_1 (\gamma_2 H_1)^{2k} e^{(2k+1)j\omega t} - H_{-1} (\gamma_2 H_{-1})^{2k} e^{-(2k+1)j\omega t} \right]$$

$$\times (-2)^k \left[1 + 2|\gamma_2 H_1|^2 + \sqrt{1 + 4|\gamma_2 H_1|^2} \right]^{-k},$$

$$+ \mu_0 \gamma_3 j\omega \left(H_1 e^{j\omega t} - H_{-1} e^{-j\omega t} \right)$$

Thus, the magnetic field B can be reconstructed as follows:

$$B = \int \frac{\partial B}{\partial t} dt + C,$$

Finally,

$$\begin{aligned}\frac{\partial B}{\partial t} &= \mu_0 \left(\frac{\gamma_1\gamma_2}{1+(\gamma_2 H)^2} + \gamma_3 \right) \frac{\partial H}{\partial t} \\ &= \mu_0\gamma_1\gamma_2 \frac{\sqrt{1+4|\gamma_2 H_1|^2}-1}{2|\gamma_2 H_1|^2} \\ &\times \sum_{k=0}^{\infty} j\omega \left[H_1(\gamma_2 H_1)^{2k} e^{(2k+1)j\omega t} - H_{-1}(\gamma_2 H_{-1})^{2k} e^{-(2k+1)j\omega t} \right] \\ &\times (-2)^k \left[1 + 2|\gamma_2 H_1|^2 + \sqrt{1+4|\gamma_2 H_1|^2} \right]^{-k}, \\ &+ \mu_0\gamma_3 j\omega \left(H_1 e^{j\omega t} - H_{-1} e^{-j\omega t} \right)\end{aligned}$$

Thus, the magnetic field B can be reconstructed as follows:

$$B = \int \frac{\partial B}{\partial t} dt + C,$$

where

Finally,

$$
\begin{aligned}
\frac{\partial B}{\partial t} &= \mu_0 \left(\frac{\gamma_1 \gamma_2}{1 + (\gamma_2 H)^2} + \gamma_3 \right) \frac{\partial H}{\partial t} \\
&= \mu_0 \gamma_1 \gamma_2 \frac{\sqrt{1 + 4|\gamma_2 H_1|^2} - 1}{2|\gamma_2 H_1|^2} \\
&\times \sum_{k=0}^{\infty} j\omega \left[H_1 (\gamma_2 H_1)^{2k} e^{(2k+1)j\omega t} - H_{-1} (\gamma_2 H_{-1})^{2k} e^{-(2k+1)j\omega t} \right] \\
&\times (-2)^k \left[1 + 2|\gamma_2 H_1|^2 + \sqrt{1 + 4|\gamma_2 H_1|^2} \right]^{-k}, \\
&+ \mu_0 \gamma_3 j\omega \left(H_1 e^{j\omega t} - H_{-1} e^{-j\omega t} \right)
\end{aligned}
$$

Thus, the magnetic field B can be reconstructed as follows:

$$
B = \int \frac{\partial B}{\partial t} dt + C,
$$

where

$$
C : \quad \lim_{H \to 0} B = 0
$$

Finally,

$$
\begin{aligned}
\frac{\partial B}{\partial t} = \mu_0 \left(\frac{\gamma_1 \gamma_2}{1 + (\gamma_2 H)^2} + \gamma_3 \right) \frac{\partial H}{\partial t} \\
&= \mu_0 \gamma_1 \gamma_2 \frac{\sqrt{1 + 4|\gamma_2 H_1|^2} - 1}{2|\gamma_2 H_1|^2} \\
&\times \sum_{k=0}^{\infty} j\omega \left[H_1 (\gamma_2 H_1)^{2k} e^{(2k+1)j\omega t} - H_{-1} (\gamma_2 H_{-1})^{2k} e^{-(2k+1)j\omega t} \right] \\
&\times (-2)^k \left[1 + 2|\gamma_2 H_1|^2 + \sqrt{1 + 4|\gamma_2 H_1|^2} \right]^{-k}, \\
&+ \mu_0 \gamma_3 j\omega \left(H_1 e^{j\omega t} - H_{-1} e^{-j\omega t} \right)
\end{aligned}
$$

Thus, the magnetic field B can be reconstructed as follows:

$$
B = \int \frac{\partial B}{\partial t} dt + C,
$$

where

$$
C : \quad \lim_{H \to 0} B = 0 \quad \Longrightarrow \quad C = 0.
$$

Effective permeability.

As a result,

$$B(t) = \sum_{k=0}^{\infty} \left\{ \mu_{2k+1}^{\text{eff}} H_1 e^{j(2k+1)\omega t} + \overline{\mu}_{2k+1}^{\text{eff}} H_{-1} e^{-j(2k+1)\omega t} \right\} .$$

Effective permeability.

As a result,

$$B(t) = \sum_{k=0}^{\infty} \left\{ \mu_{2k+1}^{\text{eff}} H_1 e^{j(2k+1)\omega t} + \overline{\mu}_{2k+1}^{\text{eff}} H_{-1} e^{-j(2k+1)\omega t} \right\}.$$

For the basic harmonic:

$$\mu_1^{\text{eff}} = \mu_0 \left[\gamma_1 \gamma_2 \frac{\sqrt{1 + 4|\gamma_2 H_1|^2} - 1}{2|\gamma_2 H_1|^2} + \gamma_3 \right].$$

And for the rest of harmonics:

$$\mu_{2k+1}^{\text{eff}} = \mu_0 \gamma_1 \gamma_2 \frac{\sqrt{1 + 4|\gamma_2 H_1|^2} - 1}{2|\gamma_2 H_1|^2}$$

$$\times \frac{(-2)^k (\gamma_2 H_1)^{2k}}{(2k+1) \left[1 + 2|\gamma_2 H_1|^2 + \sqrt{1 + 4|\gamma_2 H_1|^2} \right]^k}$$

Magnetization curves for different harmonics.

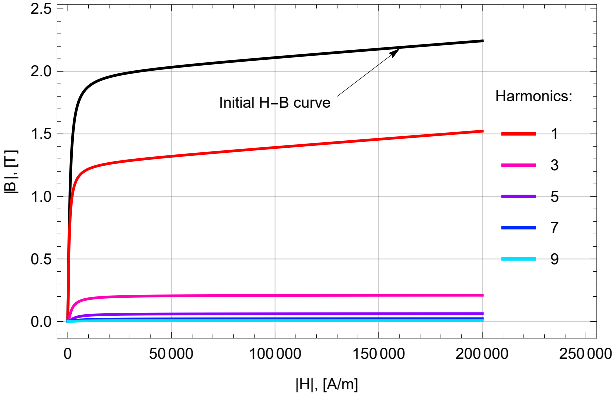

Figure 23: Magnetization curves for different harmonics

Magnetic field inside the tank wall

$$\begin{cases} \frac{1}{r}\frac{\partial}{\partial r}\left(r\frac{\partial H}{\partial r}\right) + \frac{\partial^2 H}{\partial z^2} - \frac{H}{r^2} - \beta^2 H = f(H), \\ H(r, \pm h/2) = \frac{I}{2\pi r}, \\ H(a, z) = \frac{I}{2\pi a}, \end{cases}$$

where $\beta^2 = j\omega\sigma\mu_0(\gamma_1\gamma_2 + \gamma_3) = j\omega\sigma\mu_0 \times 1001.64$,

$$f(z) = -j\omega\sigma\mu_0\gamma_1\gamma_2 \frac{1 + 2(\gamma_2|H|)^2 - \sqrt{1 + 4(\gamma_2|H|)^2}}{2(\gamma_2|H|)^2} H$$
$$\sim -j\omega\sigma\mu_0\gamma_1\gamma_2^3|H|^2 H$$

$$\gamma_1 = 999637.86\,\mathrm{A/m}$$
$$\gamma_2 = 0.001002\,(\mathrm{A/m})^{-1}$$
$$\gamma_3 = 1.0861$$

Solution to the nonlinear problem

$$H(r,z) = H_{\mathrm{lin}}(r,z) + \int_{-h/2}^{h/2}\int_a^b G(r,\rho;z-\zeta) f\big(H(\rho,\zeta)\big)\rho d\rho d\zeta,$$

Solution to the nonlinear problem

$$H(r,z) = H_{\mathrm{lin}}(r,z) + \int_{-h/2}^{h/2} \int_a^b G(r,\rho;z-\zeta) f\big(H(\rho,\zeta)\big)\rho d\rho d\zeta,$$

where the solution to the linear problem:

$$H_{\mathrm{lin}}(r,z) = \frac{I}{2\pi a}\left\{ \frac{a}{r}\frac{\cosh(\beta z)}{\cosh(\beta h/2)} + \frac{4\beta^2}{\pi}\sum_{n=0}^{\infty}\frac{(-1)^n}{\lambda_n^2(2n+1)}\frac{K_1\left(\lambda_n r\right)}{K_1\left(\lambda_n a\right)}\cos\left(\frac{\pi(2n+1)}{h}z\right)\right\},$$

Solution to the nonlinear problem

$$H(r,z) = H_{\text{lin}}(r,z) + \int_{-h/2}^{h/2}\int_a^b G(r,\rho;z-\zeta)f\big(H(\rho,\zeta)\big)\rho d\rho d\zeta,$$

where the solution to the linear problem:

$$H_{\text{lin}}(r,z) = \frac{I}{2\pi a}\Bigg\{\frac{a}{r}\frac{\cosh(\beta z)}{\cosh(\beta h/2)} + \frac{4\beta^2}{\pi}\sum_{n=0}^{\infty}\frac{(-1)^n}{\lambda_n^2(2n+1)}\frac{K_1(\lambda_n r)}{K_1(\lambda_n a)}\cos\left(\frac{\pi(2n+1)}{h}z\right)\Bigg\},$$

Green's function:

$$G(r,\rho;z) = \frac{2}{h}\sum_{n=0}^{\infty}\Bigg\{\frac{I_1(\lambda_n a)}{K_1(\lambda_n a)}K_1(\lambda_n r)K_1(\lambda_n \rho) - K_1(\lambda_n r)I_1(\lambda_n \rho)\theta(r-\rho) - K_1(\lambda_n \rho)I_1(\lambda_n r)\theta(\rho - r)\Bigg\}\cos\left(\frac{\pi(2n+1)}{h}z\right)$$

Solution to the nonlinear problem

In a symbolic form:

$$\mathbf{H} = \mathbf{H}_{\text{lin}} + \mathbf{G} \cdot f\big(\mathbf{H}\big).$$

Iterations:

$$\mathbf{H}_{n+1} = \mathbf{H}_{\text{lin}} + \mathbf{G} \cdot f\big(\mathbf{H}_n\big), \qquad \mathbf{H}_0 = \mathbf{H}_{\text{lin}}.$$

$$\text{If} \quad \exists \lim_{n\to\infty} \mathbf{H}_n, \quad \lim_{n\to\infty} \mathbf{H}_{n+1} = \mathbf{H}_{\text{lin}} + \mathbf{G} \cdot f\big(\lim_{n\to\infty} \mathbf{H}_n\big).$$

Convergence. Contraction mapping theorem:

$$\exists\, q < 1 : \quad \|\mathbf{H}_{n+1} - \mathbf{H}_n\| \le \|\mathbf{G}\| \cdot \|f\big(\mathbf{H}_n\big) - f\big(\mathbf{H}_{n-1}\big)\|$$
$$< q\,\|\mathbf{H}_n - \mathbf{H}_{n-1}\|, \text{where} \quad \|\mathbf{H}_n\| = \sup_{\substack{r\in[a,b]\\ z\in[-h/2,h/2]}} |H(r,z)|.$$

Magnetic field penetration into the tank wall. Nonlinear problem

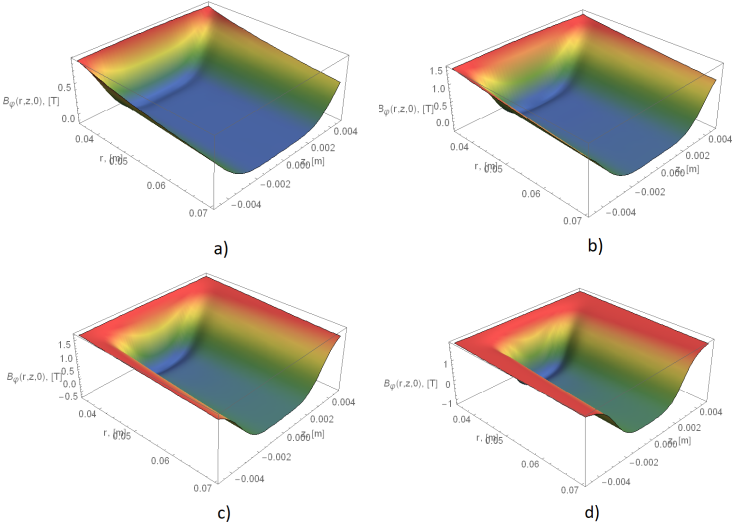

Figure 24: Wave forms of magnetic flux density: a) 176.77 A, b) 500 A, c) 1000 A, d) 1500 A.

Magnetic field penetration into the tank wall. Analytical solution vs. FEM

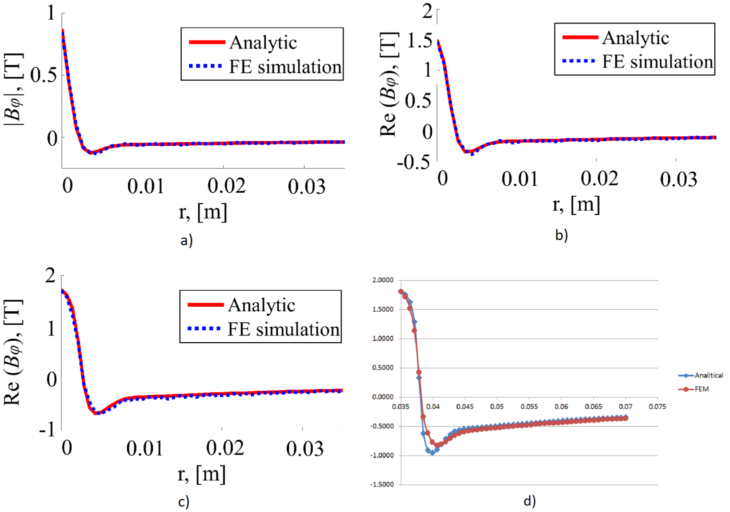

Figure 25: Analytical solution vs. FEM: a) 176.77 A, b) 500 A, c) 1000 A, d) 1500 A.

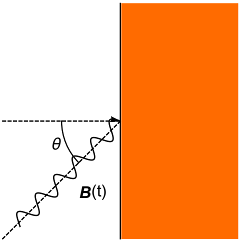

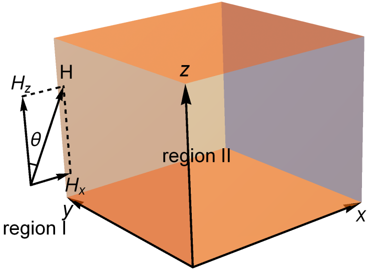

$$\mathbf{H} = H_x(x)\mathbf{e}_x + H_z(x)\mathbf{e}_z.$$

$$\gamma_2\mathbf{H} = \mathbf{h} = h_x\mathbf{e}_x + h_z\mathbf{e}_z.$$

$$\mu_{\mathrm{r}}(|\mathbf{h}|) = \gamma_1\gamma_2\frac{\sqrt{1+4|\mathbf{h}|^2}-1}{2|\mathbf{h}|^2} + \gamma_3,$$

where

$$|\mathbf{h}| = \sqrt{h_x^2 + h_z^2}.$$

Maxwell's equations yield:

$$\frac{d^2 h_z}{dx^2} = j\omega\sigma\mu_0\mu_{\mathrm{r}}(|\mathbf{h}|)h_z, \qquad (1)$$

$$\frac{d}{dx}\left\{\mu_{\mathrm{r}}(|\mathbf{h}|)h_x\right\} = 0. \qquad (2)$$

Eqs. (1) and (2) are coupled through $\mu_{\mathrm{r}}(|\mathbf{h}|)$.
Boundary conditions are:

$$h_z|_{\mathrm{II}} = h_z|_{\mathrm{I}} \equiv \mathfrak{a}_z,$$
$$\mu_{\mathrm{r}}(|\mathbf{h}|)h_x|_{\mathrm{II}} = h_x|_{\mathrm{I}} \equiv \mathfrak{a}_x.$$

Integral of Eq. (2):

$$\mu_{\mathrm{r}}(|\mathbf{h}|)h_x = \mathrm{const} = \mathfrak{a}_x,$$

wherefrom

$$h_x(x) = \frac{\mathfrak{a}_x}{\dfrac{2\gamma_1\gamma_2\left(1-\left(|\mathfrak{a}_x|/\gamma_1\gamma_2\right)^2\right)}{1+\sqrt{1+4|h_z(x)|^2\left(1-\left(|\mathfrak{a}_x|/\gamma_1\gamma_2\right)^2\right)}} + \gamma_3}.$$

Analysis of asymptotic behavior

$$\frac{d^2 h_z}{dx^2} = j\omega\sigma\mu_0\mu_\mathrm{r}(h_z)h_z,$$

$$\mu_\mathrm{r}(h_z) = \frac{2\gamma_1\gamma_2\left(1 - \left(|\mathfrak{a}_x|/\gamma_1\gamma_2\right)^2\right)}{1 + \sqrt{1 + 4|h_z|^2\left(1 - \left(|\mathfrak{a}_x|/\gamma_1\gamma_2\right)^2\right)}} + \gamma_3.$$

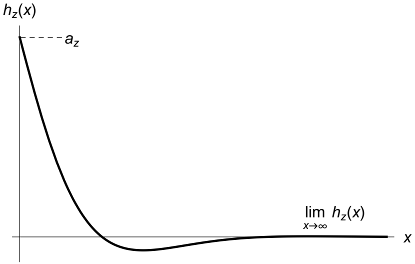

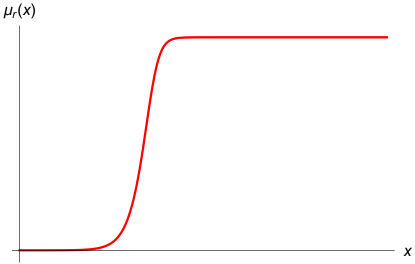

Analysis of asymptotic behavior

Near the surface ($x \to 0$)

$$\frac{d^2 h_z}{dx^2} = 2j\alpha_{\mathrm{s}}^2 h_z,$$

$$\alpha_{\mathrm{s}} = \sqrt{\frac{\omega\sigma\mu_0\mu_{\mathrm{s}}}{2}}.$$

Asymptotic solution:

$$h_z(x) \sim e^{-(1+j)\alpha_{\mathrm{s}} x}.$$

In the limit $x \to \infty$:

$$\frac{d^2 h_z}{dx^2} = 2j\alpha_\infty^2 h_z,$$

$$\alpha_\infty = \lim_{x\to\infty} \sqrt{\frac{\omega\sigma\mu_0\mu_{\mathrm{eff}}\left(|h_z(x)|\right)}{2}}$$

$$= \sqrt{\alpha_0^2 + \alpha_1^2},$$

$$\alpha_0 = \sqrt{\frac{\omega\sigma\mu_0\gamma_1\gamma_2}{2}\left(1 - \left(|\mathfrak{a}_x|/\gamma_1\gamma_2\right)^2\right)},$$

$$\alpha_1 = \sqrt{\frac{\omega\sigma\mu_0\gamma_3}{2}}.$$

Asymptotic solution:

$$h_z(x) \sim e^{-(1+j)\alpha_\infty x}.$$

Analysis of asymptotic behavior

Searching for the solution **in the first approximation** in the form:

$$h_z(x) = \mathfrak{a}_z e^{-(1+j)\alpha x}, \quad \text{where} \quad \alpha_{\mathrm{s}} < \alpha < \alpha_\infty,$$

where $h_z(x)$ satisfies the equation **in average**:

$$\frac{d^2 h_z}{dx^2} = j\omega\sigma\mu_0\mu_{\mathrm{r}}(h_z)h_z \quad \Longrightarrow$$

$$\Longrightarrow \quad \int_0^\infty \left|\frac{d^2 h_z}{dx^2}\right| dx = \int_0^\infty \Big|j\omega\sigma\mu_0\mu_{\mathrm{r}}(h_z)h_z\Big| dx.$$

$$\alpha^2 = \frac{\omega\sigma\mu_0}{2} \frac{\displaystyle\int_0^\infty \mu_{\mathrm{r}}\left(|\mathfrak{a}_z|e^{-\alpha x}\right)e^{-\alpha x}dx}{\displaystyle\int_0^\infty e^{-\alpha x}dx}$$

$$= 2\alpha_0^2 \frac{\sqrt{A}\sinh^{-1}\left(\sqrt{A}\right) + 1 - \sqrt{1+A}}{A} + \alpha_1^2,$$

where

$$A = 4|\mathfrak{a}_z|^2 \left(1 - \left(|\mathfrak{a}_x|/\gamma_1\gamma_2\right)^2\right).$$

Asymptotic solution

$$\frac{d^2 h_z}{dx^2} - 2j\alpha^2 h_z = j\left(\omega\sigma\mu_0\mu_{\mathrm{r}}(h_z) - 2\alpha^2\right) h_z,$$

where, according to the analyzed asymptotic behavior,

$$h_z(x) = h_{\mathrm{I}z}\exp\big(-(1+j)\alpha x + \psi(x) + o(\psi)\big),$$
$$\psi(0) = 0, \quad \text{and} \quad \lim_{x\to\infty} |\psi(x)| < \infty.$$

$$\psi'' - 2(1+j)\alpha\psi' = 2j\left(\alpha_0^2 \frac{2}{\sqrt{1+Ae^{-2\alpha x}}+1} + \alpha_1^2 - \alpha^2\right).$$

Solution for $\psi(x)$:

$$\psi(x) = (1+j)\frac{\left(\alpha^2-\alpha_\infty^2\right)x}{2\alpha} - \frac{\alpha_0^2}{\alpha^2}\frac{2+j}{20z}\Bigg\{8-4j+5z-(10-2j)\sqrt{1+z}$$
$$-(6+2j)z\ln\frac{1+\sqrt{1+z}}{2} + 2(1+j)F\left(j,\frac{1}{2};1+j;-z\right)\Bigg\}\Bigg|_{z=Ae^{-2\alpha x}}^{z=A},$$

Hypergeometric function

$$F(a,b;c;z) = 1 + \sum_{m=1}^{\infty} \left(\prod_{n=0}^{m-1} \frac{(a+n)(b+n)}{(c+n)} \right) \frac{z^m}{m!}$$

$$= 1 + \frac{ab}{c}\frac{z}{1!} + \frac{a(a+1)b(b+1)}{c(c+1)}\frac{z^2}{2!} + \dots .$$

Some particular cases:

$$e^z = \lim_{k\to\infty} F\left(1, k; 1; \frac{z}{k}\right),$$

$$\cos(z) = \lim_{a,b\to\infty} F\left(a, b; \frac{1}{2}; -\frac{z^2}{4ab}\right),$$

$$\ln(1+z) = z\,F(1,1;2;-z)$$

$$F\Big(j, \frac{1}{2}; 1+j; -z\Big) = 1 + \sum_{n=1}^{\infty} \frac{(-1)^n(2n-1)!}{2^{2n-1} n!(n-1)!} \frac{jz^n}{n+j}.$$

Magnetic field penetration into magnetic slab. $\theta = 0^\circ$

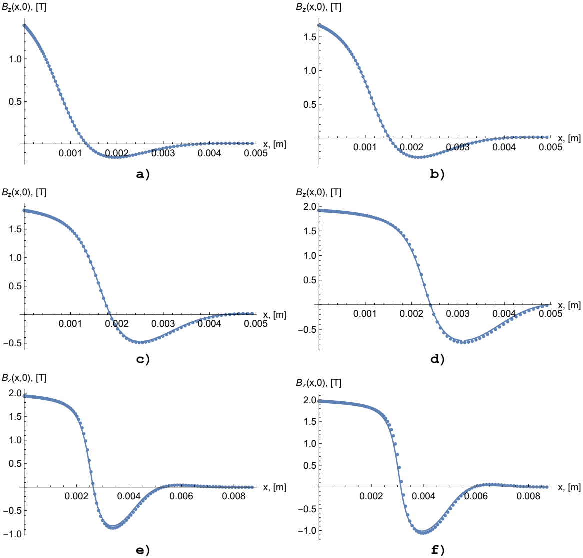

Figure 26: a) $|\mathbf{H}_\mathrm{I}| = 1000$ A/m, b) $|\mathbf{H}_\mathrm{I}| = 2000$ A/m, c) $|\mathbf{H}_\mathrm{I}| = 4000$ A/m, d) $|\mathbf{H}_\mathrm{I}| = 8000$ A/m, e) $|\mathbf{H}_\mathrm{I}| = 10000$ A/m, f) $|\mathbf{H}_\mathrm{I}| = 15000$ A/m

Magnetic field penetration into magnetic slab. $\theta = 45^\circ$

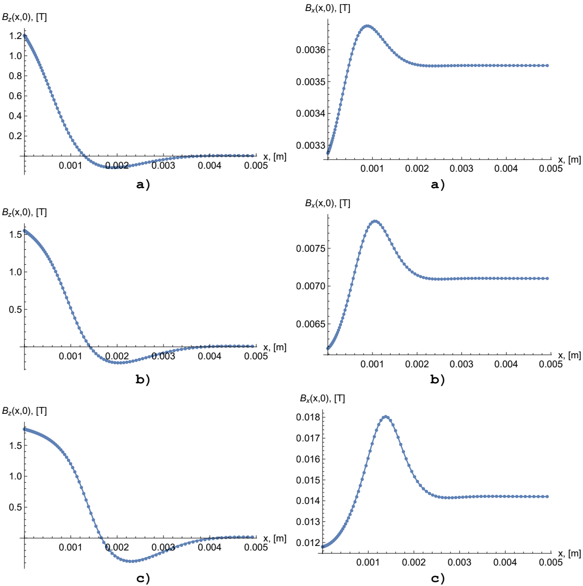

Figure 27: a) $|\mathbf{H}_\mathrm{I}| = 1000$ A/m, b) $|\mathbf{H}_\mathrm{I}| = 2000$ A/m, c) $|\mathbf{H}_\mathrm{I}| = 4000$ A/m

Magnetic field penetration into magnetic slab. $\theta = 45^{\circ}$

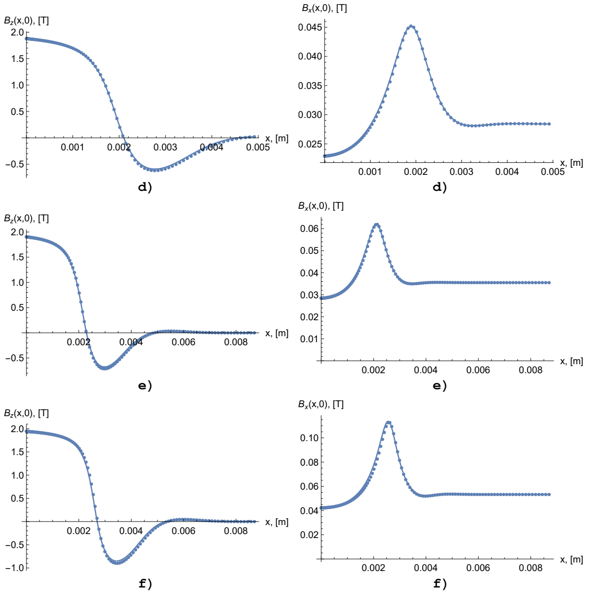

Figure 28: d) $|\mathbf{H}_{\mathrm{I}}| = 8000$ A/m, e) $|\mathbf{H}_{\mathrm{I}}| = 10000$ A/m, f) $|\mathbf{H}_{\mathrm{I}}| = 15000$ A/m

Surface impedance

Total magnetic flux per meter below the slab surface in the tangential direction:

$$\Phi = \int_0^\infty B_z(x)dx = \mu_0 \int_0^\infty \mu_\mathrm{r}(|\mathbf{H}(x)|)H_z(x)dx.$$

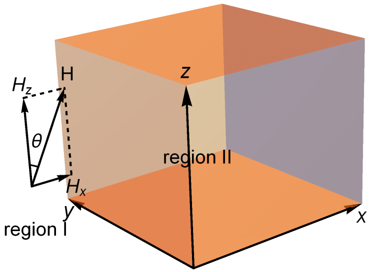

Electromotive force in the tangential direction:

$$\mathcal{E} = j\omega\Phi.$$

Current density in the tangential direction:

$$J_y(x) = -\frac{\partial H_z(x)}{\partial x}.$$

Total surface current per meter:

$$I = \int_0^\infty J_y(x)dx = H_{\mathrm{I}z}.$$

Surface impedance

Surface impedance:

$$Z_s = \frac{\mathcal{E}}{I} = \frac{j\omega\mu_0}{H_{\mathrm{I}z}} \int_0^\infty \mu_{\mathrm{r}}(|\mathbf{H}(x)|) H_z(x) dx.$$

$$Z_s = \frac{1}{2\alpha\sigma} \left\{ (1+j)\left(\alpha^2 + \alpha_1^2\right) - \frac{4\alpha_0^2}{5A} \left(5 - 2(2+j)\sqrt{1+A} \right.\right.$$
$$\left.\left. -(1-2j)\, F\left(j, \frac{1}{2}; 1+j; -A\right)\right)\right\}.$$

For Further Reading I

S. Maximov, J. C. Olivares-Galvan, S. Magdaleno-Adame, R. Escarela-Perez, E. Campero-Littlewood.
New Analytical Formulae for Electromagnetic Field and Eddy Current Losses in Bushing Regions of Transformers.
IEEE Transactions on Magnetics, 51(4):6300710, 2015.

S. Maximov, R. Escarela-Perez, S. Magdaleno-Adame, J. C. Olivares-Galvan, E. Campero-Littlewood.
Calculation of Nonlinear Electromagnetic Fields in the Steel Wall Vicinity of Transformer Bushings.
IEEE Transactions on Magnetics, 51(6):6300811, 2015.

S. Maximov, R. Escarela-Perez, J. C. Olivares-Galvan, J Guzman, E. Campero-Littlewood.
New Analytical Formula for Temperature Assessment on Transformer Tanks.
IEEE Transactions on Power Delivery, 31(3):1122-1131, 2016.

For Further Reading II

R. Escarela-Perez, S. Maximov, J. C. Olivares-Galvan, E. Melgoza, M. A. Arjona.
Effective Nonlinear Surface Impedance of Conductive Magnetic Slabs.
IEEE Transactions on Magnetics, 53(5):6300212, 2017.

D. Cahue-Diaz, S. Maximova, R. Escarela-Perez, J.C. Olivares-Galvan, J. Alvarez-Ramirez.
Effective Nonlinear Surface Impedance of Conductive Magnetic Slabs.
IEEE Transactions on Magnetics, 53(5):6300212, 2017.